EAN 2020
58th conference on experimental stress analysis

Influence of Position in 3D Printing Process on Mechanical Properties of Metal Prints

KRYSTEK J.[1,a], KAŇÁKOVÁ S.[1,b], KROUPA T. [1,c], ZEMČÍK R. [1,d], ZIKMUND, P. [2,e], ROUS, P.[3,f], STEINER, F.[3,g], VAŇKOVÁ T. [1,h]

[1]NTIS – New Technologies for the Information Society, Faculty of Applied Sciences, University of West Bohemia, Technická 8, 301 00, Plzeň, Czech Republic

[2]METAL 3D, s.r.o., Dobříš 1989, 263 01 Dobříš, Czech Republic

[3]University of West Bohemia, Faculty of Electrical Engineering, Regional Innovation Centre for Electrical Engineering (RICE), Univerzitní 8, 301 00 Plzeň, Czech Republic

[a]krystek@kme.zcu.cz, [b]kanaksan@kme.zcu.cz, [c]kroupa@kme.zcu.cz, [d]zemcik@kme.zcu.cz, [e]petr.zikmund@metal3d.cz, [f]rousp@ket.zcu.cz, [g]steiner@ket.zcu.cz, [h]vankovat@kme.zcu.cz

Keywords: Experiment, Metal 3D print, Tensile test, computed tomography

Abstract. This paper researches the influence of the placement during the 3D printing process on the quality of the final product. The tensile tests were carried out on standard dog-bone specimens, which were printed both horizontally or vertically with three orientation angles 0°, 45°, 90° to the main direction of the plate. The main goal of the measurements was to determine the influence of the printing orientation and placement of the specimens on the mechanical properties. Obtained data were evaluated and used for the determination of the best printing orientation.

Introduction

The growing popularity of 3D printing and its availability significantly influenced the manufacturing process. Nowadays, an application of 3D printing technology is immense, from products with simple decorative purposes to medical implants as shown in [1], or even whole buildings [2]. However, this technology also presents many aspects that can potentially affect the mechanical properties of the final product, e.g. a printing layer thickness, the orientation of the product against the printing equipment or a curing process.

The *Renishaw AM250* machine with the 200 W fiber laser and argon atmosphere were used. Printing parameters were developed by Metal 3D s.r.o. to get the best possible homogeneity and minimal deformation after the process of cutting the specimens from the base plate [4, 5]. Pure stainless steel powder with spherical particles was used. It was produced with gas atomization to get the desired shape of particles.

At the beginning of the process, the build chamber is closed, vacuumed and filled with argon 5.0 to get less than 1000 ppm of oxygen. The build file consists of several hundreds of layers. The whole build is made layer by layer. The base plate is stepping down in 50 µm steps, while a special mirror device is taking care of precise laser beam guidance, during the printing process. Every layer has its own parameters and strategy which the beam follows. As soon as the chamber is ready and the build file is loaded, the building starts. The base plate is covered with the powder, which is then melted with the laser. Next, the coating process follows as soon as the base plate moves down for another 50 µm. This is how the process continues until the maximum part height is reached.

X-ray tomography, also known as computed tomography (CT), allows capturing spatially large objects with their internal structure in the required accuracy. The use of X-ray technology in the form of film shots of two-dimensional images has been used in medicine for a long time. Instruments for medical 3D-tomography have been offered since the 1970s. In the early 1990s, X-ray tomography began to be used also for the inspection of technical objects, i.e. non-destructive diagnostics.

The use of CT allows checking whether there are any cracks, voids, and any other inhomogeneities, anomalies or disturbances in specimens. The second area of application is metrology. By means of CT it is possible to determine the dimensions of individual parts of analyzed objects. These dimensions (3D model) can be further compared with other samples (e.g. "gold" sample). Software tools for computed tomography provide the possibility of comparison with models created in CAD systems.

This work investigates the influence of a specimen's orientation and placement during the printing process. Thin bone-shaped specimens were placed throughout the whole base plate and printed in two ways (plane perpendicular to the thickness direction is parallel or perpendicular to the base plate, further these types of printing will be designated also as horizontal or vertical) with three different orientations made of *316L stainless steel*. The capabilities of using computed tomography scan to verify print quality have been tested.

The aim of this work was to analyze Young's modulus dependency on the specimens' position, the printing orientation, and specimens' placement on the base plate. A similar problem was presented in [3] for Polylactic Acid thermoplastic material. In the cited article, the printing orientation notably influenced the tensile strength, its value increased with increasing of the printing angle, measured from the transverse axis of the specimen.

The obtained results will be used during the future printing processes, determining the best printing position of designed products.

Tensile test

The experimental specimens were made from *316L stainless steel* (15 - 45 microns particle distribution) with a layer thickness of 50 μm, using a chessboard strategy. The 3D printing of the specimens was performed in cooperation with company Metal 3D s.r.o. The experimental specimens (Fig. 1) were printed horizontally (the specimens LA, LB and LC) and vertically (SA, SB, SC) with three orientation angles 0°, 45°, 90° throughout the whole area of the base plate. All specimens were made at one build plate with production time exceeding 30 hours. Additional 14 hours were used for a wire EDM cutting to remove the specimens from the base plate. A traditional cheaper and faster band saw could be used, but the aim was for a precise cut. At the last step the remaining supporting structures were removed.

Geometric parameters (width W and thickness H) and weight M of the specimens are presented in Table 1. Total length of specimens was $L = 100$ mm. Specimens were prepared according to ASTM E8 / E8M Standard Test Methods for Tension Testing of Metallic Materials. The specimens were exposed to a tensile quasi-static loading in the longitudinal direction. The loading velocity of the crosshead was $v = 1$ mm/min and temperature was $T = 21$ °C. The universal testing machine *Zwick/Roell Z050* was used. A uniaxial extensometer was used for measuring the elongation (the gage length was $L_0 = 10$ mm). The force–displacement dependencies were obtained from the tensile test. The stress–strain dependencies (Fig. 2) were calculated using

$$\sigma = \frac{F}{W \cdot H}, \quad and \quad \varepsilon = \frac{\Delta L}{L_0}. \tag{1}$$

The elastic modulus was identified on the interval of stress $\sigma \in \langle 250{,}300 \rangle\, MPa$. Elastic modulus, yield strength and ultimate stress (strength of material) are presented in Table 2.

The influence on the resulting mechanical properties of the way the specimens were 3D printed was found. Horizontally printed specimens have higher values of elastic modulus, yield strength and maximum stress than vertically printed specimens (Table 2).

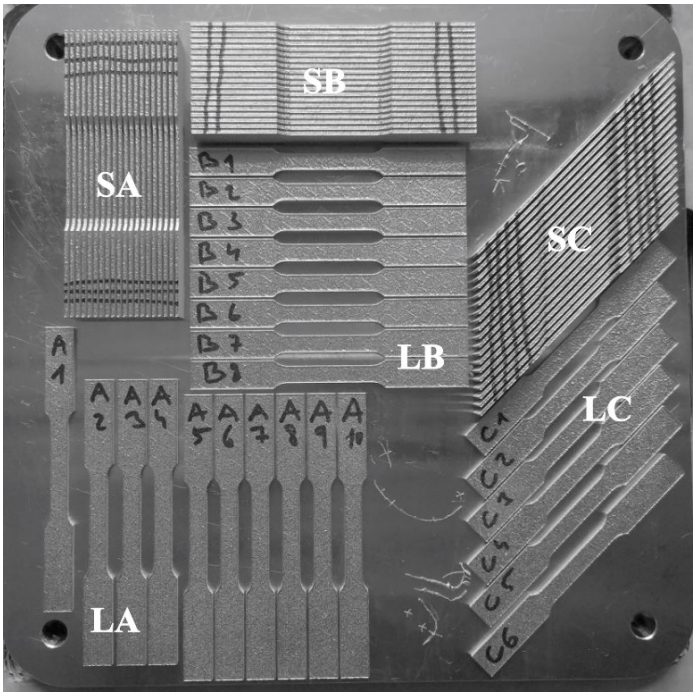

Fig. 1: The placement of each specimen

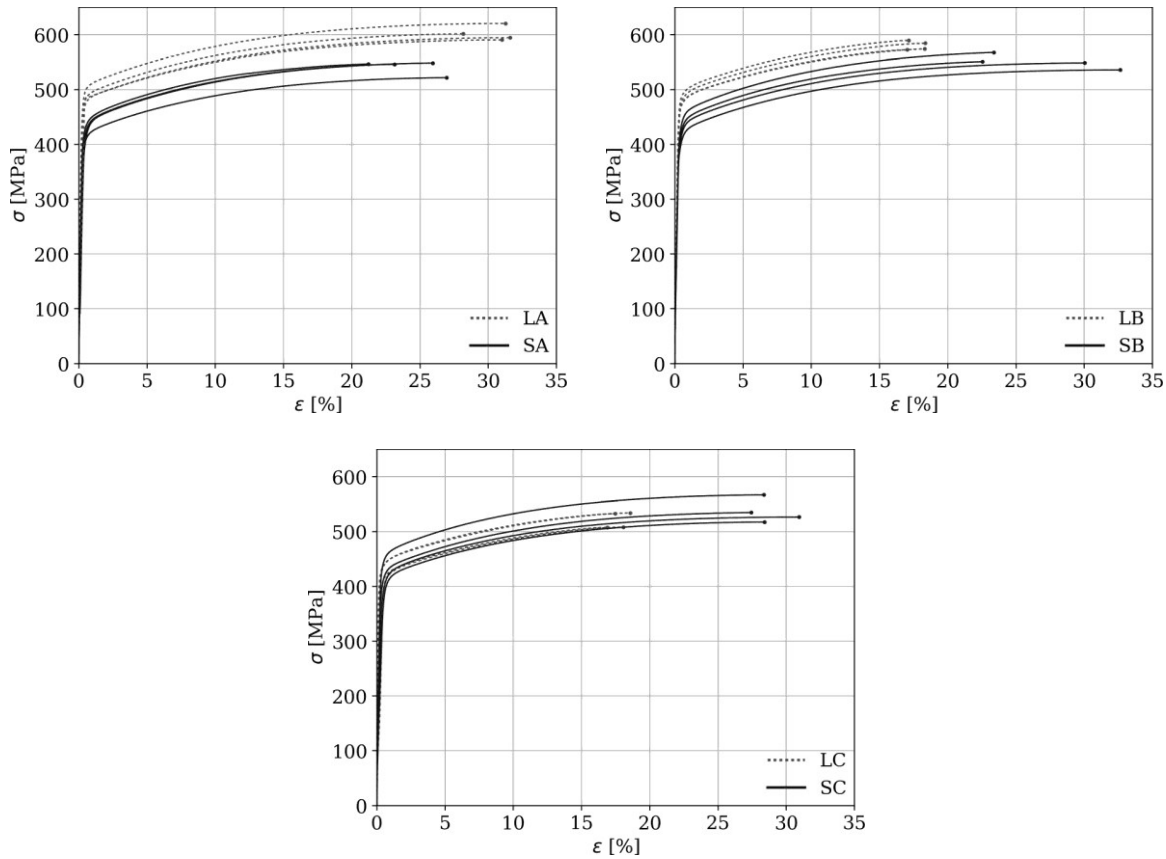

Fig. 2: Stress–strain dependencies

Table 1: Geometric parameters and weight of specimens

Specimen name	W [mm]	H [mm]	M [g]	Specimen name	W [mm]	H [mm]	M [g]
LA_1	6.14	1.17	7.158	SA_1	6.40	1.24	7.207
LA_2	6.20	1.16	6.889	SA_2	6.48	1.22	7.182
LA_3	6.17	1.16	6.935	SA_3	6.57	1.28	7.220
LA_4	6.19	1.25	7.635	SA_4	6.55	1.22	7.252
LB_1	6.16	1.29	7.519	SB_1	6.42	1.21	7.252
LB_2	6.14	1.29	7.550	SB_2	6.41	1.28	7.281
LB_3	6.13	1.26	7.576	SB_3	6.53	1.23	7.321
LB_4	6.16	1.28	7.624	SB_4	6.61	1.23	7.286
LC_1	6.24	0.97	5.579	SC_1	6.42	1.29	6.994
LC_2	6.25	0.99	5.718	SC_2	6.30	1.28	7.135
LC_3	6.19	0.96	5.627	SC_3	6.37	1.30	7.094
LC_4	6.18	0.98	5.701	SC_4	6.36	1.31	7.115

Table 2: Elastic modulus (E), yield strength ($Rp_{0.2}$), ultimate strength (σ_{max})

Specimen name	E [GPa]	$Rp_{0.2}$ [MPa]	σ_{max} [MPa]	Specimen name	E [GPa]	$Rp_{0.2}$ [MPa]	σ_{max} [MPa]
LA_1	140	495	621	SA_1	114	424	546
LA_2	121	487	591	SA_2	94	422	549
LA_3	178	478	595	SA_3	116	407	522
LA_4	155	483	602	SA_4	110	432	547
mean value	148.5	485.8	602.3	mean value	108.5	421.3	541.0
coefficient of variation [%]	14.1	1.3	2.0	coefficient of variation [%]	8.0	2.2	2.1
LB_1	152	472	574	SB_1	121	438	570
LB_2	134	474	573	SB_2	112	404	536
LB_3	163	485	590	SB_3	130	425	551
LB_4	112	480	585	SB_4	121	421	549
mean value	140.3	477.8	580.5	mean value	121.0	422.0	551.5
coefficient of variation [%]	13.8	1.1	1.3	coefficient of variation [%]	5.3	2.9	2.2
LC_1	105	414	509	SC_1	134	441	567
LC_2	123	413	508	SC_2	114	413	535
LC_3	165	433	533	SC_3	99	411	527
LC_4	132	435	535	SC_4	75	401	518
mean value	131.3	423.8	521.3	mean value	105.5	416.5	536.8
coefficient of variation [%]	16.6	2.5	2.5	coefficient of variation [%]	20.5	3.6	3.5

Computed tomography

A Phoenix v|tome|x s 240 inspection equipment was used for analysis. The device is equipped with a 240 kV 320 W micro-focal open X-ray tube and 180 kV high-performance nano-focal X-ray tube. The computed tomography system with a conical X-ray source enables inspection of samples up to 260 mm in diameter, 420 mm in height and 10 kg in weight with a high resolution of up to 1 µm.

Fig. 3: Phoenix v|tome|x s 240 inspection equipment - 240 kV 320 W micro-focal open X-ray tube and 180kV high-performance nano-focal X-ray tube

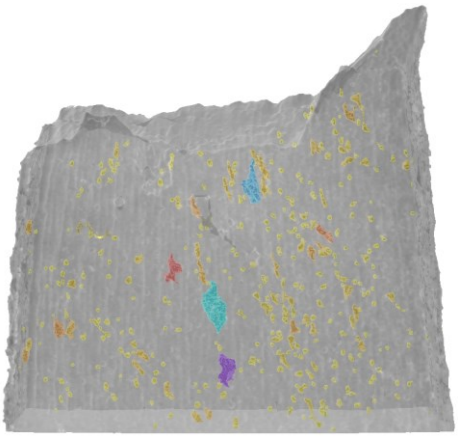

Fig. 4: Defect distribution for specimen LA_1 after tensile test

After scanning the 3D model, it is also necessary to analyze the acquired data. *VGSTUDIO MAX* (high-end software for analysis and visualization of CT data) was used. In order to obtain the necessary information, the extension module of the system (Porosity / Inclusion Analysis Module) was used.

Specimens LA_1 (after tensile test) and LA_10 (non-tested in tensile test) were analyzed by means CT. A defect value ratio of specimen LA_1 (v_d = 0.44 %) was 4 times greater than specimen LA_10 (v_d = 0.11 %).

Conclusions

The influence on the resulting mechanical properties of the way the specimens were 3D printed was found. Horizontally printed specimens have higher values of elastic modulus, yield strength and maximum stress than vertically printed specimens. It is worth to note, that specimens, whose longitudinal axis is not parallel to any of the edges of the base plate also show the lowest values of mechanical properties. Furthermore, the capabilities of the computed tomography were shown.

Future work will be aimed at finding a correlation between mechanical properties and volume fraction, spatial distribution and/or orientation of the voids in the 3D printed specimens. This will need a new set of specimens with more suitable dimensions for CT scanning.

Acknowledgement

This publication was supported by the project LO1506 of the Czech Ministry of Education, Youth and Sports and project of the Technology Agency of the Czech Republic no. TN1000007 (subproject no. 1, segment no. 1, working package no. 5).

References

[1] A. Jíra, P. Hájková, L. Řehounek, Trabecular structures as efficient surface of dental implants, in: Proceedings of the 57th International Scientific Conference on Experimental Stress Analysis. Luhačovice, Czech Republic, 2019, pp. 169–174.

[2] I. Hager, A. Golonka, R. Putanowicz, 3D printing of buildings and building components as the future of sustainable construction?, International Conference on Ecology and new Building materials and products, ICEBMP 2016, pp. 292–299.

[3] Y. Zhao,Y. Chen, Y. Zhou, Novel mechanical models of tensile strength and elastic property of FDM AM PLA materials: Experimental and theoretical analyses, Materials and Design, Vol. 181, 5 November 2019. ISSN 0264-1275.

[4] V. Novotny, M. Vitvarova, M. Kolovratnik, B. B. Stunova, V. Vodicka, J. Spale, P. Zikmund, M. Drasnar, and E. Schastlivtseva. Design and Manufacturing of a Metal 3D Printed kW Scale Axial Turboexpander, in: Proceedings of the ASME Turbo Expo 2019: Turbomachinery Technical Conference and Exposition. Volume 8: Microturbines, Turbochargers, and Small Turbomachines; Steam Turbines. Phoenix, Arizona, USA, 2019. https://doi.org/10.1115/GT2019-91822

[5] V. Novotny, J. Spale, B. B. Stunova, M. Kolovratnik, M. Vitvarova and P. Zikmund, 3D Printing in Turbomachinery: Overview of Technologies, Applications and Possibilities for Industry 4.0, in: Proceedings of the ASME Turbo Expo 2019: Turbomachinery Technical Conference and Exposition. Volume 6: Ceramics; Controls, Diagnostics, and Instrumentation; Education; Manufacturing Materials and Metallurgy. Phoenix, Arizona, USA, 2019. https://doi.org/10.1115/GT2019-91849